

# Downlink transmit diversity schemes for CDMA networks

J.S.Thompson, P.M.Grant and B.Mulgrew

**Abstract:** Transmit diversity schemes that have been proposed for the downlink in CDMA networks are discussed. They provide diversity gain against Rayleigh fading at the mobile which can significantly improve performance. Theoretical error formulas for convolutional codes are shown to be useful in optimising the performance of some of these techniques. Performance results from a number of simulation studies are also presented. These can be used to determine the strengths and weaknesses of the algorithms and their effect on a typical CDMA network. The effects of Rician fading and fast downlink power control on transmit diversity are discussed.

## 1 Introduction

Recently, cellular networks based on code division multiple access (CDMA) technology have been deployed across the world, particularly in America and Asia (for more details see [1]). CDMA systems offer a number of advantages, such as universal frequency reuse, soft handoff on both links and the ability to trade voice quality for increased capacity. However, some form of power control is usually required on both links to minimise multiple access interference (MAI) between different users in the system.

Early analyses of CDMA networks based on the IS-95 standard, e.g. [2], suggested that the capacity of such a system was limited by that achievable on the uplink. However, a number of more recent studies have indicated that this is not necessarily the case [3, 4]. One reason for this is that dual space diversity is always available on the uplink, while on the downlink a slow moving mobile operating in a flat Rayleigh fading channel observes little or no diversity. Secondly, the update rate of power control is significantly higher on the uplink than the downlink. These effects can lead to large  $E_s/N_0$  requirements on the downlink. The capacity of the downlink is determined by the maximum transmit power available at the cell site, so that large  $E_s/N_0$  values will limit capacity. Therefore if the  $E_s/N_0$  requirement of all mobiles can be reduced, the downlink capacity will be increased.

This paper discusses transmit diversity (TD) techniques that use two diversity antennas to provide improved performance on the downlink. A number of different techniques have been proposed which provide different means for the mobile to exploit the diversity available from the transmitters. Delay diversity [5] and phase sweeping [6] provide diversity through the creation of a time-selective or frequency-selective fading channel. Delay diversity can be

viewed as a specific case of space-time coding, which is discussed and analysed in [7]. None of these techniques involve the transmitter requiring access to information about the downlink channel condition. Alternatively, it is possible to exploit a feedback path from the mobile to the base-station to adjust the transmitter waveforms. Analysis of such techniques may be found in [8]. TD schemes in general have also been analysed from an information theoretic point of view and the results of this work may be found in [9] and the references therein.

Transmit diversity can be compared with soft handoff [3], which is a macro-diversity technique. Soft handoff provides diversity gain to all mobiles in the handoff area and also reduces the downlink shadow margin, since the shadow fading processes observed from the different base stations are usually partially decorrelated. Unlike soft handoff, TD is unable to reduce the shadow margin, because it is not a macro-diversity technique. However, TD does provide diversity gain to all mobiles in the network, whereas the effectiveness of soft handoff is limited to those mobiles which observe multiple pilot signals of comparable strength. In addition, soft handoff uses up resources at multiple base stations, which can become a limiting factor on system capacity.

## 2 Channel and receiver model

A single-user transmission is considered on the downlink of an IS-95 based system. This choice has been made for reasons of simplicity. However, a number of the TD schemes discussed here have been proposed for use in 3G CDMA systems, such as cdma2000 [10] or UTRA [11]. Many of these schemes cannot be applied directly to existing IS-95 systems without altering the IS-95 standards specifications. However, the performance comparisons that are obtained here should also apply to 3G CDMA systems, except for small differences due to the coding scheme, interleaver structure, etc.

In this Section, only the parts of the transmitter necessary for simulation are described. For full details of the IS-95 base station transmitter, see [12]. The user's baseband binary data  $d(t)$  is first encoded using a rate  $r = 1/2$ , constraint length  $K_c = 9$  convolutional code, whose generators are octal 753 and 561. The coded output of one frame

© IEE, 2000

IEE Proceedings online no. 20000689

DOI: 10.1049/ip-com:20000689

Paper first received 1st June 1999 and in revised form 6th April 2000

The authors are with the Signals and Systems Group, Department of Electronics and Electrical Engineering, The University of Edinburgh, Kings Buildings, Edinburgh EH9 3JL, UK

of 192 data bits (384 codeword bits) is then subject to interleaving to produce the binary sequence  $c(t)$ . (The last  $K_c - 1$  data bits of the frame are zeros, to ensure that the coder returns to the all-zeros state at the frame end.) Fifty frames are transmitted per second, so the gross data rate is 9.6 kbit/s. This sequence is then modulated by the user's Walsh code  $w_u(t)$  and then by a complex outer spreading code  $p(t)$ . For the purpose of base station identification and coherent demodulation, a coherent pilot signal is transmitted with the user's signal using Walsh code  $w_0(t)$ .

The transmitted waveform may thus be written as

$$x(t) = p(t) [c(t)A_t w_u(t) + A_p w_0(t)] \exp\{j2\pi f_C t\} \quad (1)$$

where  $f_C$  is the carrier frequency,  $A_t$  is the traffic channel amplitude and  $A_p$  denotes the amplitude of the pilot signal. This waveform is transmitted over a multipath channel to the desired mobile. The channel may be modelled using an  $L$  tap delay line, whose impulse response is given by

$$h(t) = \sum_{l=1}^L h_l(t) \delta(t - lT_c)$$

where  $h_l(t)$  is the  $l$ th channel tap coefficient,  $\delta(t)$  denotes the Dirac delta function and  $T_c$  is the chip period of the spreading sequence  $p(t)$ . The received signal at the mobile is simply the convolution of  $x(t)$  with  $h(t)$ . This waveform is demodulated to baseband; the result may be written as

$$\begin{aligned} y(t) = & \sum_{l=1}^L h_l(t) p(t - (l-1)T_c) \\ & \times [A_t c(t - (l-1)T_c) w_u(t - (l-1)T_c) \\ & + A_p w_0(t - (l-1)T_c)] + v(t) \end{aligned}$$

The notation  $v(t)$  denotes additive thermal noise.

The receiver is modelled according to a number of assumptions

(A1) The Gaussian noise process  $v(t)$  is spectrally flat over the bandwidth of the receiver.

(A2) The channel coefficients  $h_l(t)$  vary slowly with time with a maximum Doppler rate  $f_D$ . The RF channel does not vary over one symbol period  $T_s$ , so that  $f_D \ll 1/T_s$ .

(A3) The channel coefficients  $h_l(t)$  are modelled using one of two candidate statistical distributions:

- In most cases, all coefficients  $h_l(t)$  follow the classical Doppler fading model and have a Rayleigh distribution. The correlation function of this fading process is  $R(\Delta t) = J_0(2\pi f_D \Delta t)$ , where  $J_0(x)$  is the zero-order Bessel function of the first kind.

- A Rician fading model will also be considered for the first received channel tap ( $l = 1$ ). The direct path component has a Doppler frequency of  $0.7f_D$ , so that the correlation function becomes  $R(\Delta t) = x_1 J_0(2\pi f_D \Delta t) + x_2 \exp(j1.4\pi f_D \Delta t)$ . The  $K$ -factor of this distribution is equal to the ratio  $(x_2/x_1)$ .

(A4) The correlation properties of the spreading code  $p(t)$  are assumed to be ideal, so that self-noise interference between the  $L$  multipath components of the traffic and pilot channels is neglected here.

To determine the  $l$ th multipath component for the  $n$ th codeword bit, the receiver performs the following operation:

$$D(l, n) = \frac{1}{T_s} \int_0^{T_s} y(\tau + (n-1)T_s + (l-1)T_c) \cdot$$

$$\begin{aligned} & \times p^*(\tau + (n-1)T_s) w_u(\tau + (n-1)T_s) d\tau \\ & = A_t h_l(n) c(n) + n_l(n) \end{aligned} \quad (2)$$

The notation  $p^*(t)$  denotes the complex conjugate of  $p(t)$ . Assumptions (A1) and (A4) mean that interference term  $n_l(n)$  consists only of thermal white Gaussian noise of zero mean and variance  $\sigma^2$ . Further, it is assumed that  $A_t = 1$  for a single antenna transmitter, so that the SNR of  $D(l, n)$  depends only on  $h_l(n)$  and  $n_l(n)$ .

To proceed, the receiver must determine the unknown channel coefficients  $h_l(n)$ . This is done by measuring the pilot signal, i.e. substituting  $w_0(t)$  in place of  $w_u(t)$  in eqn. 2 and re-evaluating the integral. The result, denoted as  $P(l, n)$ , provides the required channel amplitude and phase. It is assumed that the pilot amplitude  $A_p$  is sufficiently large to provide a noise-free estimate of the channel. The receiver forms a soft decision on the  $n$ th codeword bit by maximal ratio combining of the  $L$  multipath components as follows:

$$S(n) = \sum_{l=1}^L \Re\{P^*(l, n) D(l, n)\} \quad (3)$$

The notation  $\Re$  denotes the real part of a complex number; it is used here because coherent PSK demodulation is employed. The soft decisions  $S(n)$  of one frame of data are then de-interleaved and passed to a Viterbi decoder. The decoder contains the trellis of the convolutional code and it determines the most likely transmitted sequence of transmitted data symbols for that frame.

## 2.1 Performance bound on convolutional codes

The performance of the downlink is assessed in terms of the frame error ratio (FER), where an FER of 1% or less is assumed to be satisfactory. (In real CDMA networks, the target FER may be increased slightly to increase capacity or reduced slightly to improve voice quality. However, this will not significantly affect the algorithm comparisons presented in this paper.) Each frame contains a cyclic redundancy check (CRC), which is used to detect whether a frame error has occurred. It is assumed that the CRC correctly detects all frame errors. A performance bound called the 'error probability per node' ([13], section 4.4) indicates the likelihood of selecting an incorrect code trellis path at each stage of decoding. The FER is then given by the probability that at least one node error occurs during the frame.

The error probability for node  $k$  using a rate 1/2 convolutional code, under the channel assumptions above, is given by

$$P_e(k) \leq \sum_{d=d_f}^{\infty} \sum_{i=1}^{a_d} P_d(i, k) \quad (4)$$

where the coefficient  $a_d$  is the number of decoder paths with Hamming distance  $d$  from the true path (usually taken as the all 0s path, for simplicity). The scalar  $d_f$  denotes the minimum Hamming distance of the code under consideration. The function  $P_d(i, k)$  is the probability that for the  $i$ th distinct path which diverges at node  $k$  with overall Hamming distance  $d$ , the metric of that path is better than the all 0s path when they merge together again at node  $k + l$ .

The function  $P_d(i, k)$  may be evaluated by determining the metrics of the two competing paths, summed over the  $2l$  codeword bits

$$M_0 = \sum_{q=0}^{2l} S(n_q) \quad M_i = \sum_{q=0}^{2l} S(n_q) c(i, n_q)$$

where  $c(i, n)$  denotes the  $n$ th (interleaved) codeword bit for the  $i$ th path. The notation  $n_q$  is used to indicate the position of the  $q$ th codeword bit in the sequence  $c(n)$ , after interleaving. The probability that  $M_0 < M_i$  is simply given by

$$\begin{aligned} P_d(i, k) &= \Pr\{M_0 - M_i < 0\} \\ &= \Pr\left\{\left(\sum_{q=1}^{2l_i} S(n_q)[1 - c(i, n_q)]\right) < 0\right\} \\ &= \Pr\left\{\left(\sum_{q=1}^d 2S(n_q^d)\right) < 0\right\} \end{aligned} \quad (5)$$

The notation  $n_q^d$  denotes the interleaved position of the  $q$ th coded bit in which the two competing paths differ. The form of eqn. 5 is equivalent to the probability of error for coherent PSK modulation with maximal ratio combining of the  $d$  differing codeword bits. In the case of Rayleigh fading, the value of  $P_d(i, k)$  is given by the standard result ([14], p. 802)

$$P_d(i, k) = \frac{1}{2} \sum_{l=1}^{N_D} \left( \prod_{\substack{q=1 \\ q \neq i}}^{N_D} \frac{\gamma_l}{\gamma_l - \gamma_q} \right) \left[ 1 - \sqrt{\frac{\gamma_l}{1 + \gamma_l}} \right] \quad (6)$$

This result assumes the eigenvalues  $\gamma$  are all different. This can easily be extended to the case of multiple equal and unequal eigenvalues as shown in [15]. The quantities  $\gamma$  are the set of all  $N_D$  non-zero eigenvalues obtained from the  $L$  size  $d \times d$  covariance matrices  $H(l)$ . Using the correlation function  $R(\Delta l)$  defined in assumption (A3), the  $x$ th row and  $y$ th column entry of  $H(l)$  is

$$\begin{aligned} H(l)_{xy} &= E[h_l(n_x^d)h_l^*(n_y^d)] / \sigma^2 \\ &= \frac{\rho_l}{\sigma^2} R([n_y^d - n_x^d] T_s) \\ &= \frac{\rho_l}{\sigma^2} J_0(2\pi f_D [n_y^d - n_x^d] T_s) \end{aligned} \quad (7)$$

The notation  $\rho_l$  denotes the mean signal power of the  $l$ th tap and  $E[\cdot]$  is the expected value. Equivalent closed-form results for  $P_d$  in the Rician fading case appear to be harder to obtain. Two alternatives are to use the Chernoff bound [7] or a Gaussian noise channel approximation to Rician fading [16].

To facilitate evaluation of eqns. 4 and 6, three simplifying assumptions are made, the first two following the ideas of [17].

(A5) Only the minimum Hamming distance paths, where  $d = d_f$ , are considered in the summation term for  $P_e$  (denoted as method A). For the convolutional code,  $d_f = 12$  and there are  $a_{12} = 11$  paths with this distance. The effect of considering only the shortest minimum distance path ( $l_i = 9$  nodes) will be addressed as well, denoted as method B.

(A6) To avoid implementing specific details of the code for method A or B, it is assumed that the  $d_f$  differing bits are spread uniformly over the path length of  $2l_i$  coded bits. This means that the matrices  $\{H(l)\}$  are always of size  $2l_i$ ; the resulting eigenvalues  $\gamma$  are scaled by  $d_f/2l_i$  to obtain the correct  $E_b/N_0$  value in the evaluation of  $P_e$ .

(A7) The value of  $P_e$  has been evaluated for node  $k = 1$  in an IS-95 frame. There was found to be negligible difference in the results obtained by this approach and by averaging the value of  $P_e$  obtained for all possible nodes  $k$  within one frame. Even without these simplifying assumptions, this bound may be rather loose for the case of fading channels.

This is because it considers each competing path in isolation: in practice, when a fade occurs there are likely to be many paths with better metrics than the correct all zeros path. However, using these simplifications, eqn. 6 provides a means to compare the diversity gain provided by different realisations of TD schemes, which will be found subsequently to be useful.

### 3 Transmit diversity techniques

The basic channel model for TD is introduced here. All the schemes assume that  $M = 2$  widely spaced diversity antennas are located at the base station. (It is also possible to exploit polarisation diversity.) This number has been chosen since dual diversity provides a large proportion of the gain available from diversity techniques. Using two antennas also minimises the complexity increase required and matches the space diversity configuration typically used on the uplink. To provide a fair comparison to a single antenna transmitter,  $A$ , is reduced from 1 to  $1/\sqrt{2}$  for each diversity antenna in eqn. 1. This means that the total transmitter power across all antennas is the same in both cases.

Both antennas have an  $L$ -tap multipath channel to the mobile, whose  $l$ th coefficient is denoted as  $h_{lm}(n)$ ,  $m = 1$  or 2. The assumption of large antenna spacing means that  $E[h_{l1,m1}(n)h_{l2,m2}^*(n)] = 0$ , provided that  $l1 \neq l2$  or  $m1 \neq m2$ . This paper considers seven candidate schemes for TD on the downlink. Unless otherwise stated, the two antennas use two different orthogonal Walsh codes for the pilot signals, so that both antennas' channels can be estimated at the receiver. Each scheme considers how the model of the previous Section, in particular eqns. 2, 3 and 6, are modified to model that particular scheme.

#### Space time transmit diversity (STTD)

STTD is a recently proposed scheme [18] that doubles the order of receive diversity for all coded symbols while using the same traffic channel Walsh code at both antennas. (An alternative scheme, codeword diversity (CWD), uses two different traffic channel Walsh codes at the two antennas. This latter scheme is more wasteful of Walsh codes than STTD. However, if the mobile tracks the  $L$  channel taps for both Walsh codes, order  $2L$  diversity is again obtained for all coded bits. CWD was found to have identical performance to STTD for all the simulation scenarios considered in Section 4.2.) Consider the coded bit pair  $c(n)$  and  $c(n+1)$ . For the  $n$ th bit period, the coded bits  $c(n)$  and  $-c(n+1)^*$  are transmitted from antennas 1 and 2; at time  $n+1$ ,  $c(n+1)$  and  $c(n)^*$  are transmitted. The  $l$  multipath components are measured using eqn. 2 as normal. Finally, the soft decisions for the  $n$ th and  $(n+1)$ th coded bits are obtained as

$$\begin{aligned} S(n) &= \sum_{l=1}^L \Re\{P_1^*(l, n)D(l, n) \\ &\quad + P_2(l, n)D^*(l, n+1)\} \\ S(n+1) &= \sum_{l=1}^L \Re\{P_1^*(l, n)D(l, n+1) \\ &\quad - P_2(l, n)D^*(l, n+1)\} \end{aligned}$$

The notation  $P_1$  and  $P_2$  denote pilot measurements from the two antennas. These equations assume that the channel does not change from symbol  $n$  to  $(n+1)$ . Provided this assumption is true, no signal component for  $c(n+1)$  is present in  $S(n)$  and vice-versa. The effect of STTD is that the soft decisions  $S(n)$  consist of maximal ratio combining

of all  $2L$  channel coefficients  $\{h_{l,1}\}$  and  $\{h_{l,2}\}$ . The effect of this on eqn. 6 is that each nonzero eigenvalue  $\gamma$  is divided by two (due to the transmit power being split between two antennas) and its multiplicity doubled.

#### *Delay diversity (DD)*

In this scheme the same pilot channel and traffic channel Walsh codes are used at both antennas. A time delay of  $L$  CDMA code chips is applied to the signal  $x(t)$  at the second antenna to generate an artificial multipath channel containing  $2L$  channel taps [5]. In principle, the method can also provide order  $2L$  diversity for all coded bits. Thus, ignoring self-noise, its performance should be the same as that for STTD and CWD. However, the multipath channel destroys the orthogonality of Walsh codes for all users in the cell. The multiple access interference that is created will worsen the performance of DD relative to STTD and CWD.

#### *Orthogonal transmit diversity (OTD)*

OTD is a technique which bears some similarity to STTD, but using a different order of symbol transmission for the two antennas ([10], p. 51). At time  $n$ , the coded bits  $c(n)$  and  $c(n+1)$  are transmitted; at time  $(n+1)$ , the coded bits  $c(n)$  and  $-c(n+1)$  are transmitted. This is equivalent to using two orthogonal Walsh codes which have twice the period of  $w_u(t)$ . This time, the soft decisions are obtained as

$$S(n) = \sum_{l=1}^L \Re \{ P_1(l, n) [D(l, n) + D(l, n+1)] \}$$

$$S(n+1) = \sum_{l=1}^L \Re \{ P_2(l, n) [D(l, n) - D(l, n+1)] \}$$

The  $n$ th soft decision consists of the maximal ratio combining of the  $L$  channel coefficients  $\{h_{l,1}\}$  and the  $(n+1)$ th decision combines the  $L$  coefficients  $\{h_{l,2}\}$ . To apply OTD to the IS-95 downlink, the interleaver structure was modified. The normal interleaver ([12], Chapt. 7) operates such that all odd codeword bits are sent in the first half of the frame and all even bits in the second half. For the OTD scheme, the first half of the interleaved frame was sent on antenna 1 and the second half on antenna 2. Thus the effect of OTD on the channel matrix  $H(l)$  is to modify eqn. 7 to

$$H(l)_{xy} = \begin{cases} \frac{\rho_l}{\sigma^2} J_0 (4\pi f_D [n_y^d - n_x^d] T_s) & \text{if } [n_y^d - n_x^d] \text{ is even} \\ 0 & \text{otherwise} \end{cases} \quad (8)$$

The extra factor of two present in the argument of  $J_0$  arises from the doubled period of the Walsh codes in this case. It is apparent that the diversity condition of each coded bit is not improved by OTD; instead diversity gain is provided by the convolutional decoder.

#### *Phase sweeping transmit diversity (PSTD)*

In this case, the same pilot channel and traffic channel Walsh codes are used at both antennas. A time varying phase offset term  $\exp(j2\pi f_P t)$  is applied to the second antenna's signal before transmission at RF [6]. The mobile then observes the sum of the two antennas' signals. The phase offset between the two antennas gives rise to a time-varying signal at the mobile, even in the case where there is no Doppler dispersion ( $f_D = 0$ ). If the mobile assumes a carrier frequency of  $f_C + (f_P/2)$ , the correlation function in eqn. 7 is modified to [6]

$$H(l)_{xy} = J_0 (2\pi f_D [n_y - n_x] T_s) \cos(\pi f_P [n_y - n_x] T_s)$$

#### *Time switched transmit diversity (TSTD)*

In this approach, the base station switches the desired user's traffic channel between the two antennas [19] at a rate of  $S_r$  switches per frame. This time, the value of  $H(l)_{xy}$  will be zero, unless the same antenna was active both at time  $n_x$  and  $n_y$ . In the latter case, the value of the matrix entry becomes  $J_0(2\pi f_D [n_y - n_x] T_s)$ .

#### *Selective transmit diversity (STD)*

Unlike the previous methods, STD permits the use of an information feedback path from the mobile to base station. The mobile monitors the total received power for each antenna's pilot signal. The mobile periodically signals on the uplink, at a rate of  $S$ , bits per frame, which antenna is the better one to use for its traffic channel. This information is used by the base station to select the better antenna for the given mobile [19]. Results exist in the literature [20] for  $P_d$  in the case where the fading channel is constant over a frame ( $f_D = 0$ ). However, analysis of the situation where  $f_D > 0$  is more difficult and is not pursued here. For very rapid fading channels, STD may be unable to switch antennas rapidly enough to track the fading dynamics properly. One composite scheme to overcome this drawback would employ STD only for mobiles known to be moving slowly; faster moving mobiles would use the TSTD scheme instead as this requires no feedback from the mobile.

#### *Pre-RAKE transmission*

A lower bound on the performance of all the foregoing techniques is obtained when the base station has perfect knowledge of channel coefficients  $\{h_{l,m}(n)\}$ . The mobile periodically signals the base station with the channel coefficients obtained from each transmit antenna's pilot signal. The pre-RAKE technique, which has been proposed for time-division duplex systems [21], can then be applied. An additional, user-specific pilot Walsh code should then be allocated to facilitate the mobile's channel tracking. Each antenna convolves the traffic and user-specific pilot channels with the time inverse, complex conjugate channel weights, before transmission. The receiver simply tracks the largest received multipath component, since this is the coherent sum of all multipath taps from both antennas. This scheme permits a reduction in transmit power equal to the array gain, which is  $M = 2$  (3dB), relative to STTD. Issues related to vector quantisation schemes for coefficient feedback are discussed in [8].

The STTD, OTD, TSTD, STD and pre-RAKE techniques could be used in 3G CDMA systems, provided that the mobile is configured appropriately. However, the DD and PSTD schemes could be applied to existing IS-95 networks without changing the mobile handset. In the following Section, the performance of the different techniques is compared and the impact on CDMA networks discussed.

## 4 Algorithm performance

This Section investigates the performance of TD techniques using both theoretical and simulation results. The simulator's channel and receiver models operate as described in Section 2. The system carrier frequency  $f_C = 1.8$ GHz in all simulations and mobile speeds of 5 or 50km/h are considered. The single user case is always assumed with no self-noise interference, so that the only disturbance is thermal noise. In the results below the total transmit power for the desired user's traffic channel is always the same, whether 1 or 2 transmitter antennas are used. Therefore the receiver  $E_b/N_0$  level results below are always directly proportional to the total transmitter power required by any scheme for a given FER.

#### 4.1 Optimising parameters

We consider the carrier offset frequencies  $f_p$  used in PSTD and the maximum antenna switching rate  $S_r$  for TSTD and STD. Results are verified by the IS-95 downlink simulator, using a carrier frequency of 1.8GHz. A one-tap Rayleigh fading channel is assumed with mobile speeds of 5 or 50km/h.

To determine the optimum offset frequency for PSTD, both theoretical and simulation approaches have been used. The node error probability  $P_e$  has been evaluated for Rayleigh fading to determine under what conditions it is minimised. In this case, the values of  $P_e$  for both methods A and B (as defined in assumption (A5), Section 2.1) were found to be almost identical. The results provide an indication of the values of  $f_p$  required to optimise performance. This procedure has then been validated by  $E_b/N_0$  simulation results. Fig. 1a shows the value of  $P_e$  for different PSTD offset frequencies  $f_p$  at an  $E_b/N_0$  of 10dB (this value of  $E_b/N_0$  was selected as an approximation to the exact  $E_b/N_0$  values for the two mobile speeds) and Fig. 1b shows the corresponding required  $E_b/N_0$  results from simulation.

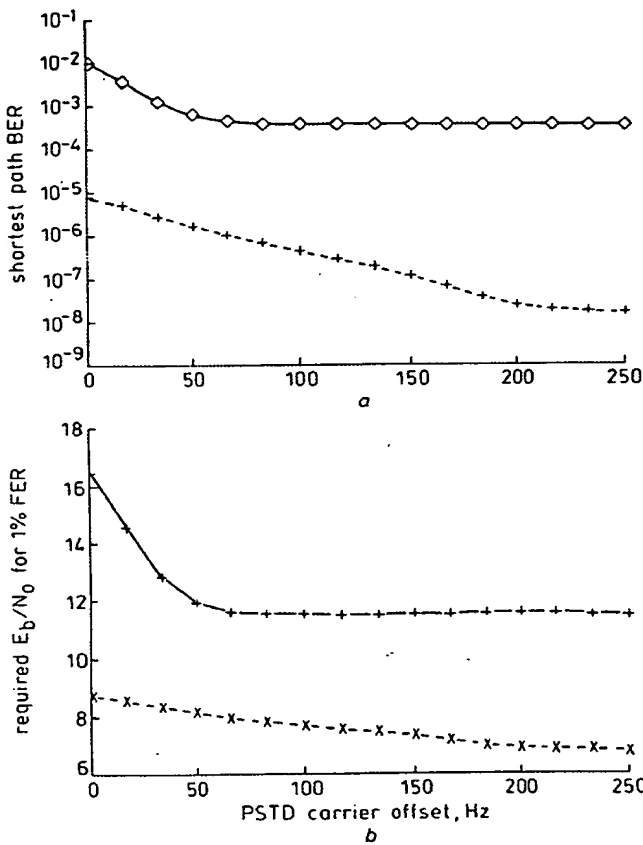


Fig. 1 Optimising PSTD for a one-tap Rayleigh fading channel, with mobile speeds of 5 and 50km/h  
 — 5km/h  
 - - - 50km/h  
 a Shortest path error probability  $P_e$  results for an  $E_b/N_0$  of 10dB  
 b Corresponding results of required  $E_b/N_0$  for an FER of 1%

The results show that the minimum value of  $P_e$  does provide a good indication of the optimum values of  $f_p$ . For a 5km/h mobile, setting  $f_p$  to about 75Hz minimises both the value of  $P_e$  and the required  $E_b/N_0$  value to about 11.5dB. Similarly for a 50km/h mobile, setting  $f_p$  to about 225Hz appears to minimise the  $E_b/N_0$  to about 6.75dB. These results show that larger carrier offsets are required for faster mobiles than is the case for slower mobiles. However, Fig. 1b shows that the performance benefit of PSTD is much less for 50km/h than for 5km/h. If an excessively

large carrier offset is selected, very high Doppler shifts will be observed at all mobiles, making channel tracking more difficult. It may be better to select a small carrier offset, such as 75Hz, at the cost of a 1dB increase in required  $E_b/N_0$  for 50km/h mobiles.

The same procedure has been used to evaluate the switching rate (measured in number of switches per frame) for TSTD. The results for  $P_e$  are shown in Fig. 2a and the corresponding  $E_b/N_0$  results in Fig. 2b. In Fig. 2a, results are shown for both methods A and B, since they diverge at a switching rate of 32 times per frame. For a mobile speed of 5km/h, switching at four times per frame seems to be sufficient to optimise performance. For a mobile speed of 50km/h, switching at 12–16 times per frame is required to achieve the lowest  $E_b/N_0$  results. These curves also show that switching at too high a rate can be counterproductive. Fig. 2a shows that method B predicts a very significant performance loss for switching at 32 times per frame. However, this seems to be a problem with the shortest path only, as method A shows a less marked increase in  $P_e$ , which is more in line with the simulation results in Fig. 2b. The fact that performance degrades when switching is increased from 16 to 32 times per frame must be due to the channel covariance matrix  $H(l)$ , defined in eqn. 7. It appears that increasing the switching rate introduces extra correlations into  $H(l)$ , which adversely affects the diversity gain for the minimum Hamming distance paths in the Viterbi decoder.

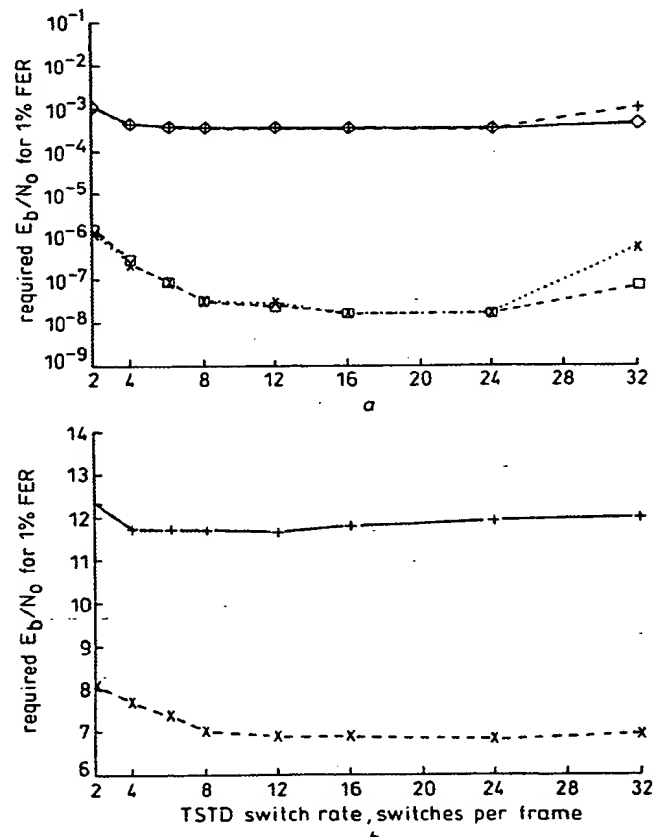


Fig. 2 Optimising TSTD switching rate (per frame) for a one-tap Rayleigh fading channel, with mobile speeds of 5 and 50km/h  
 a Shortest path error probability  $P_e$  results for an  $E_b/N_0$  of 10 dB  
 —○— A, 5km/h    —□— A, 50km/h  
 -+-- B, 5km/h    -×-- B, 50km/h  
 b Corresponding  $E_b/N_0$  results from simulation  
 — 5km/h  
 - - - 50km/h

The results for  $P_e$  obtained for PSTD and TSTD may be compared with those for OTD and STTD. For a speed of

5km/h, OTD gives  $P_e = 3.3 \times 10^{-4}$  and STTD gives  $P_e = 3.5 \times 10^{-4}$ ; for 50km/h, OTD gives  $P_e = 1.5 \times 10^{-8}$  and for STTD,  $P_e = 1.2 \times 10^{-8}$ . These match closely the best values obtained for  $P_e$  at both speeds for the PSTD and TSTD algorithms. Therefore these results suggest that all four algorithms will have similar performance. However, assumption (A6) neglects the specific structure of the convolutional codes. STTD always doubles the order of diversity on all codeword bits. PSTD, OTD and TSTD all provide extra diversity in the decoding process, so that these methods are sensitive to the specific code structure, which was neglected in assumption (A6). Therefore STTD can be expected to perform slightly better than PSTD, OTD or TSTD.

In the STD method, the value of  $P_e$  is difficult to obtain in closed form for nonzero  $f_D$ . A simpler way to determine the optimum value of  $S_r$  is to consider the channel's correlation in time. Specifically, the correlation between the following two times is considered: the time of the mobile's measurement, and the time when the last coded bit is reached before the next antenna switch could be performed. The time period between two consecutive antenna switches is called a 'subframe'. Initially, no delay in feedback process is assumed, so that the base station is informed immediately that the mobile makes a measurement. It can then instantly switch transmit antenna if required. This means that the correlation time period is then equal to one subframe.

Ideally the correlation across one subframe should be unity, so that the channel has not changed at all. However, for a finite Doppler frequency  $f_D$ , this requires  $S_r$  to be infinite. In practice we must choose a compromise value of  $S_r$ , which is large enough to ensure that the subframe correlation is close to one without requiring excessive feedback on the uplink. Fig. 3 plots the correlation function for classical Doppler fading, with the switching rate axis (measured in switches/second) normalised by the Doppler frequency  $f_D$ . The results show that correlations of 0.9 and 0.95 are achieved by  $S_r/f_D = 10$  and 14, respectively. These correlation values are sufficiently high to provide most of the performance gains available with unity correlation. If there is a delay in feeding back information about the channel, this will increase the required switching rate. For example, if there is a delay of one subframe between the mobile's measurement and the antenna switch, the correlation time period is doubled. This has the effect of doubling the required switching rate  $S_r$  to achieve the same correlation as for the zero delay case.

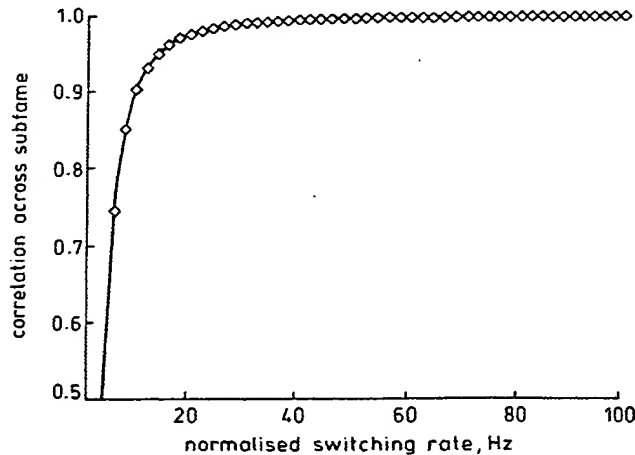


Fig. 3 Correlation function for subframe with classical Doppler fading plotted against normalised switching rate  $S_r/f_D$

Fig. 4 shows  $E_b/N_0$  results for STD method plotted against the switching rate  $S_r$  per frame. Results are shown for the cases where the feedback path has a bit error ratio (BER) of 0 or 0.1. Successive feedback path errors are modelled as independent Bernoulli random variables [22] with probability of success equal to the feedback path BER. When an error occurs, the base station selects the wrong antenna for transmission of the next subframe. Fig. 4b also includes results for the case where there is a one subframe delay in the feedback path. The mobile speeds of 5 and 50km/h correspond approximately to  $f_D = 8$  and 80Hz, respectively.

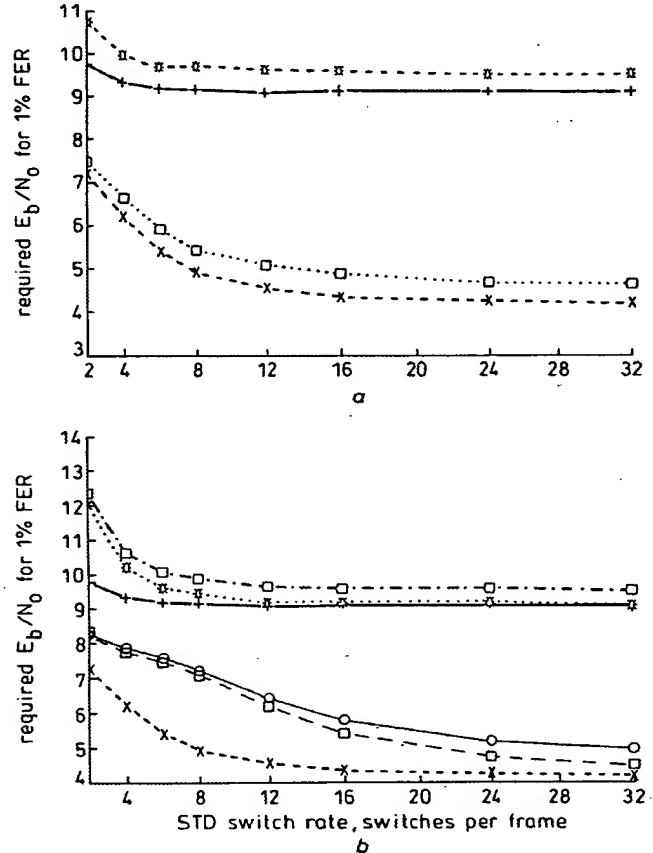


Fig. 4  $E_b/N_0$  results for STD with a one-tap Rayleigh fading channel and mobile speeds of 5 and 50km/h using a feedback path BER of 0 or 0.1

a Results with no feedback delay  
 $\text{---} + \text{---}$  5km       $\text{---} + \text{---}$  5km (BER = 0.1)  
 $\text{---} \times \text{---}$  50km       $\text{---} \square \text{---}$  50km (BER = 0.1)  
b Equivalent results for the case of one subframe delay  
 $\text{---} + \text{---}$  5km       $\text{---} \square \text{---}$  5km (BER = 0.1)  
 $\text{---} \times \text{---}$  50km       $\text{---} \square \text{---}$  50km (BER = 0.1)  
 $\text{---} + \text{---}$  1 sub-frame delay, 5km       $\text{---} \diamond \text{---}$  1 sub-frame delay, 50km

In Fig. 4a, setting  $S_r = 4$  switches per frame (i.e. 200 switches/second, which is roughly  $25f_D$ ) for a mobile speed of 5km/h and uplink BER = 0 is sufficient to accrue most of the performance gain for STD. At a mobile speed of 50km/h, setting  $S_r = 16$  (roughly  $10f_D$ ) appears to provide most of the benefit of STD. The results for BER = 0.1 show that STD is relatively insensitive to errors on the feedback path. The typical increase in  $E_b/N_0$  due to these errors is on the order of 0.5–0.75dB. However, Fig. 4b shows that feedback delay has a significant effect on performance. The curves show that including feedback delay means that  $S_r$  must be increased by 2.5–3 times to achieve the same  $E_b/N_0$  for the zero delay case. For a mobile speed of 5km/h,  $S_r$  must be increased to 12 to optimise performance. For 50km/h mobiles with  $S_r = 16$ , the  $E_b/N_0$  increases by 1dB with the delay included, and by 1.5dB when the

BER is set to 0.1 as well. Increasing  $S_r$  to 24 or 32 will improve  $E_b/N_0$ , but at the cost of increased signalling overhead on the uplink.

#### 4.2 Results for $E_b/N_0$ performance

In this subsection, the two carriers for PSTD are offset by 75 and 225Hz for mobile speeds of 5 and 50km/h, respectively. Antenna switching occurs 16 times per frame for TSTD. In the case of STD, the mobile feedback path operates at 16 bits per frame, with no delay or feedback path error effects included.

Initially, an  $L = 1$  tap Rayleigh fading channel is considered. Results are shown in Fig. 5a, plotting the FER against the total received  $E_b/N_0$  at the mobile. The results show that the pre-RAKE method performs best, achieving a gain of 8.5dB in  $E_b/N_0$  for an FER of 1%, compared to the single antenna no diversity baseline (NDB). STD provides a gain of 7dB in  $E_b/N_0$ , while the STTD method achieves about 5.5 dB gain in  $E_b/N_0$ . Finally the OTD, TSTD and PSTD methods all have similar performance, with a gain of 4-4.5dB in  $E_b/N_0$ . Fig. 5b shows the results for a  $L = 2$  equal power tap Rayleigh fading channel. The TD algorithms perform in a similar way to the  $L = 1$  case, but the gains are smaller because there is more diversity present in the channel. The pre-RAKE obtains a reduction in  $E_b/N_0$  of about 6.5dB, relative to the NDB. The STD method achieves a gain of about 4.5dB in  $E_b/N_0$ , while the other four methods achieve  $E_b/N_0$  gains of about 3-3.5dB.

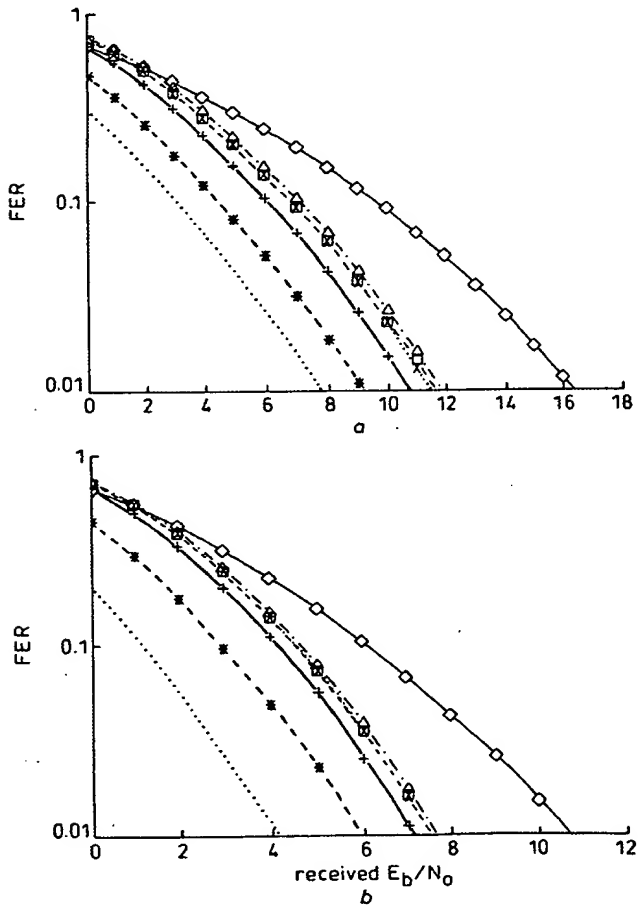


**Fig.5** Plots of FER against  $E_b/N_0$  for a single transmit antenna (NDB) and the five TD schemes

The mobile speed is 5km/h

—○— NDB    -·Δ-· TSTD  
—+— STTD    -·+-· STD  
—□— OTD    ..... pre-RAKE  
—×— PSTD

a One-tap Rayleigh fading channel

b Two-equal-power-tap Rayleigh fading channel

The results in Fig. 6 show the required  $E_b/N_0$  at the mobile to achieve 1% FER. Four Rayleigh fading channels are considered: one-tap channel, two-tap channel with the second tap 8dB weaker than the first, two equal-power-tap channel, and three equal-power-tap channel. The results in Fig. 6a show that there is a diminution in diversity gain as the amount of inherent channel diversity increases. For example, the 7.5dB gain of STD over the NDB for the one-tap case reduces to roughly 3dB for a three equal-power-tap channel. However, the relative performance of the different TD schemes does not vary significantly with the channel number. The pre-RAKE scheme is always 3 dB better than STTD, while STD is still about 1-1.5dB better for the three equal-tap channel.

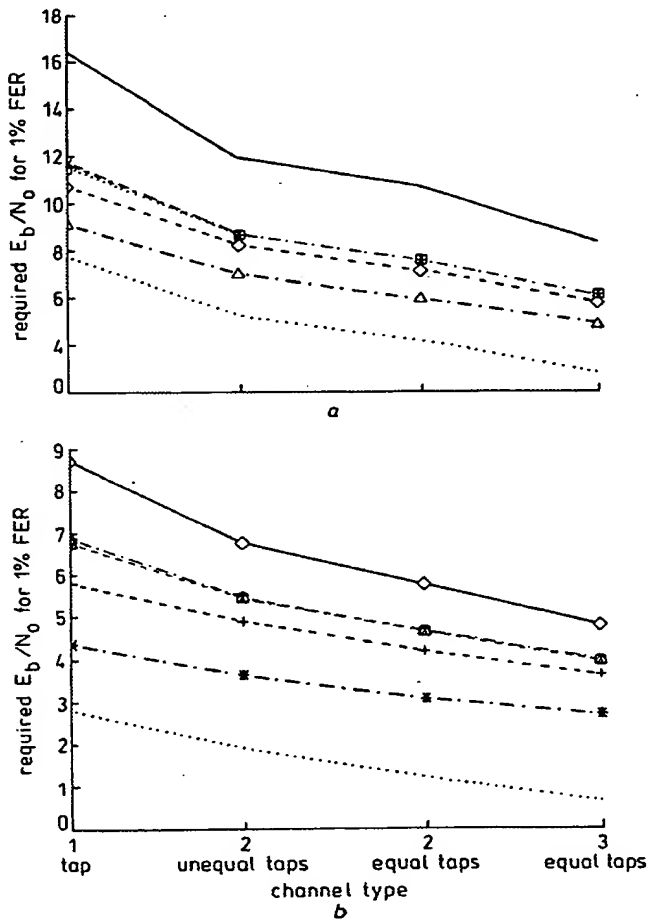


**Fig.6** Plots of required  $E_b/N_0$  for 1% FER for the different schemes for mobile speeds of 5 and 50km/h  
The four channels are 1 tap, 2 taps with powers (0, -8) dB, 2 equal power taps, and 3 equal power taps

a 5km/h	NDB	-·X-· TSTD
	—○— STTD	-·Δ-· STD
	-·+— OTD	..... pre-RAKE
	-·□— PSTD	
b 50km/h	NDB	-·Δ-· TSTD
	—+— STTD	-·+-· STD
	-·□— OTD	..... pre-RAKE
	-·X— PSTD	

The results in Fig. 6b consider a case where significantly more diversity is available to the receiver because of the fast mobile speed (50km/h). As might be expected, the improvements available from diversity gain are smaller in Fig. 6b than for Fig. 6a. For a one-tap channel, STD is now about 4.5dB better than the NDB; when a three-tap channel is considered, this reduces to only 2dB. In addition, when the effects of delay and uplink BER are included, as in Fig. 4b, STD may not perform much better than STTD or TSTD

for fast mobile speeds. The option of switching from STD to TSTD for fast mobiles only [19] will mean little performance loss while removing the requirement for an uplink feedback path. Only the pre-RAKE method is able to provide significant performance improvements, achieving a gain of 4dB even for the three-tap channel.

Assessing the impact of TD on a CDMA network is a complicated process. Some initial observations can be made using the results of Fig. 6. If the majority of users are moving at 5km/h and observe a single-tap Rayleigh fading channel, their  $E_b/N_0$  requirement can be reduced by 5.5dB using STTD for example. However, there is likely to be a mix of different user types, with different speeds and channel conditions. Also, a significant proportion of users will be in soft handoff, which ensures that they will obtain at least dual diversity. The exact proportion depends on the soft-handoff threshold  $T_{add}$ , which determines the signal-to-interference ratio that must be exceeded by a downlink pilot signal for soft handoff to occur. Simulation results presented in [3, 23] suggest that 40–60% of users should be in soft handoff to provide good cell coverage. For 5km/h mobiles, the average  $E_b/N_0$  of STTD is 3.8dB better than that for the NDB for the four channels in Fig. 6a. For 50km/h mobiles the average  $E_b/N_0$  is reduced by only 1.8dB. Averaging both results gives an improvement of 2.7dB. The improvement offered by STTD is strongly dependent on the diversity condition of mobiles in the network; the more diversity provided by the channel, the smaller the gain.

The pre-RAKE method is in theory able to improve performance by 3dB relative to the STTD method in all cases. However, this assessment is too optimistic for practical implementations. First, the pre-RAKE method is best suited to slow moving mobiles, to minimise the coefficient update required on the uplink feedback path. Secondly, the transmit power will need to increase due to the requirement for each user to have a separate pilot signal. Again, the required increase in  $E_b/N_0$  due to the pilot signal will be minimised when the mobile is moving slowly.

Finally, it is worthwhile to compare the DD and PSTD schemes directly, since they could both be used in existing IS-95 networks. In principle, DD has the same performance as STTD. However, as noted in Section 3, the DD method destroys Walsh code orthogonality and the extra multiple access interference which will arise increases the required  $E_b/N_0$ . Depending on the carrier offset  $f_P$ , the PSTD scheme will require at least 0.5–1dB extra  $E_b/N_0$  when compared to DD/STTD. However, PSTD is likely to be preferred in practice, since it does not affect the orthogonality of the Walsh code channels. Unlike DD, it also does not increase the number of multipath components that the mobile must track.

#### 4.3 Effects of Rician fading on TD schemes

Consider a case where the fading statistics are no longer Rayleigh, but follow a Rician distribution. This form of fading has an associated  $K$ -factor which is equal to the power in the line-of-sight (sine wave) component divided by the total power of the specular (Rayleigh) components. Most of the techniques described still provide improved performance because the receiver observes two independent versions of a Rician distribution with the same  $K$ -factor. Unfortunately, this does not apply in the case of PSTD, where the receiver observes the non-coherent sum of two Rician random variables with same  $K$ -factor. The increase in  $K$ -factor of the sum equals  $10 \log(1 + \cos \phi)$ , where  $\phi$  is the phase shift between the two sine wave components.

This has been plotted in Fig. 7a and shows that the  $K$  factor increase varies from 3 to  $\infty$  dB. This effect means that the performance benefit of using PSTD will not be as much for high  $K$  factor channels as for Rayleigh fading environments.

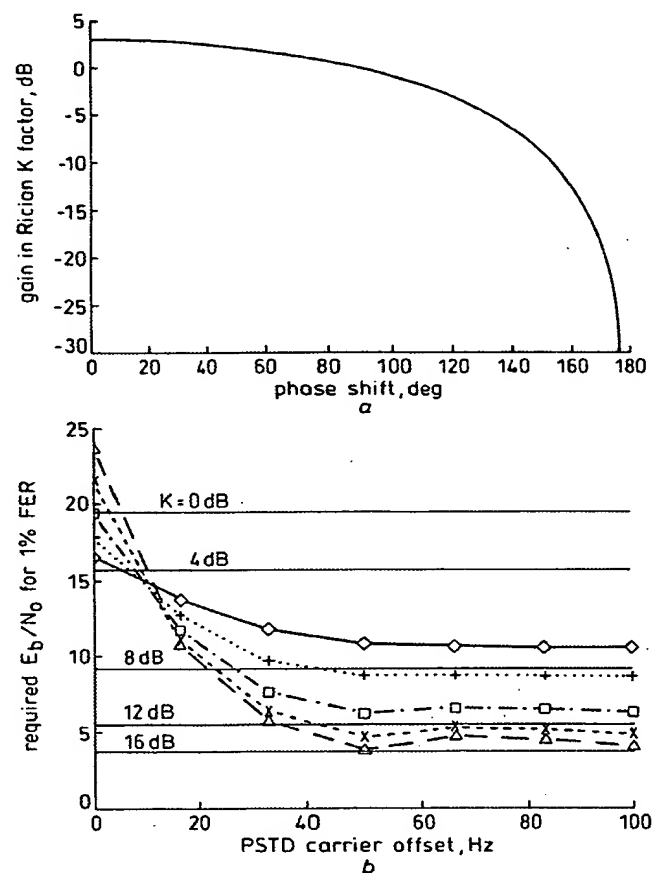


Fig. 7 K-factor and  $E_b/N_0$  for PSTD

a Increase in  $K$ -factor as a function of the relative phase between the two sine wave components

b  $E_b/N_0$  for PSTD, with a one-tap channel and an actual mobile speed of 5km/h against PSTD carrier offset  $f_P$ . The  $K$ -factor varies from 0–16dB and straight lines show the equivalent NDB results

PSTD:  
 —○—  $K = 0\text{dB}$       —×—  $K = 12\text{dB}$   
 .....+.....  $K = 4\text{dB}$       —△—  $K = 16\text{dB}$   
 - -□- -  $K = 8\text{dB}$

Fig. 7b shows  $E_b/N_0$  results for PSTD as a function of the carrier offset  $f_P$  for  $K$ -factors of 0–16dB. There is a one-tap channel and the mobile speed is 5km/h for this case. Straight lines show the  $E_b/N_0$  results for the NDB where PSTD is not applied. For low  $K$ -factor values, such as 0dB, PSTD still provides significant performance improvements over the NDB. Even when  $K = 16\text{dB}$ , using PSTD achieves almost the same  $E_b/N_0$  results as the NDB. The optimum carrier offset  $f_P$  is seen to reduce with increasing  $K$ -factor; when  $K$  is large the behaviour of the sine wave components dominates. Both components have the same Doppler frequency  $0.7f_D$ , so that for  $K = 16\text{dB}$  setting  $f_P = 50\text{Hz}$  becomes sufficient to optimise the gain of PSTD, while an offset of around 75Hz is required for  $K = 0\text{dB}$ .

#### 4.4 Effects of fast power control

Until now, the transmitter power has been fixed, and the effects of downlink power control have not been considered. Fast downlink power control has been proposed for third generation CDMA systems ([10], p. 49), so that the traffic channel amplitude  $A$ , may adapt rapidly to channel conditions. Downlink fast power control has been analysed

in [24] and is likely to operate in a similar manner to that used on the uplink of existing IS-95 systems. Fast uplink power control has been discussed in a number of papers, for example [25, 26]. It seems reasonable to apply the results obtained there to the downlink case as well. [25] specifies two major performance characteristics

(i) *For very slow mobile speeds*, where the maximum Doppler rate is much smaller than the power control update rate, shadowing and Rayleigh fading effects can be perfectly equalised. Ignoring the shadow margin, the required  $E_b/N_0$  at the receiver is essentially that for an additive white Gaussian noise channel (2.5dB for 1% FER). However, the transmit power can fluctuate significantly, as the base station tries to compensate for Rayleigh fading. Consider a downlink fading channel which is defined so that using transmit power  $B$  dB leads to a mean  $E_b/N_0$  at the mobile of  $B$  dB. For  $L$ th-order diversity, the mean transmit power and standard deviation  $\sigma_p$  can be obtained from [25] and the Appendix

$$\begin{aligned} E[P_T] &= \int_0^\infty \frac{1}{y} p_L(y) dy = \begin{cases} \infty & L = 1 \\ (BL)/(L-1) & L > 1 \end{cases} \\ \sigma_p &= \sqrt{E[P_T^2] - E[P_T]^2} \\ &= \begin{cases} \infty & L = 1, 2 \\ (BL)/((L-2)^{1/2}(L-1)) & L > 2 \end{cases} \quad (9) \end{aligned}$$

The notation  $p_L(y)$  denotes the probability density function (PDF) of the fading: with  $L$ th-order diversity it is that for an order  $2L$  chi-squared distribution. Clearly, at least dual diversity is required to avoid a requirement for infinite mean power. Also,  $L$  must be greater than two to avoid an infinite standard deviation  $\sigma_p$ . In practice there will be a finite limit on the maximum transmit power. The Appendix provides the required results for  $E[P_T]$  and  $\sigma_p$  for this case. As an example, Table 1 presents results for the transmit power statistics  $E[P_T]$  and  $\sigma_p$  with the NDB and STTD schemes for 1–3 tap Rayleigh fading channels. The results have been obtained by setting the maximum transmit power at 20dB above the set point  $B$ , so that the threshold  $T = -20$ dB. These results show that using STTD provides a significant reduction in the mean power of 4.5dB in the one-tap case. The improvement in mean power is somewhat smaller for two- and three-tap channels. However, the standard deviation  $\sigma_p$  is reduced by 4–6dB when STTD is applied in all three cases.

**Table 1: Results for PT with fast power control, with and without STTD scheme applied**

No. of taps	1	2	3
$E(P_T)$ (NDB), dB	9.9	5.4	4.2
$\sigma_p$ (NDB), dB	14.0	7.8	4.1
$E(P_T)$ (STTD), dB	5.4	3.7	3.3
$\sigma_p$ (STTD), dB	7.8	2.2	0.2
$E(P_T)$ gain, dB	4.5	1.7	0.9
$\sigma_p$ gain, dB	6.2	5.6	3.9

It is shown in [24] that the standard deviation of  $P_T$  will also affect downlink CDMA capacity. This is because the downlink capacity is usually specified in terms of the required transmitter power exceeding that available for a small percentage of the time (e.g. 2% [24]). It is apparent from the results of Table 1 that using STTD, particularly

for the one-tap case, will improve system capacity by reducing both the mean and standard deviation of the required transmit power. Ideal equalisation of Rayleigh fading is unlikely to be obtained when either PSTD or TSTD is used. Both algorithms will generate a rapidly changing channel at the mobile, even when the channel Doppler frequency  $f_D$  is zero. The fast power control algorithm has to track a much more rapidly changing channel than would be the case for STTD or OTD, for example. This will lead to a significantly higher  $E_b/N_0$  requirement for PSTD and TSTD than for other TD schemes. A worst-case analysis is obtained by assuming that the Rayleigh fading is now not equalised at all, so that the  $E_b/N_0$  results in Fig. 6a for TSTD and PSTD apply unchanged to this scenario.

(ii) *For fast mobile speeds*, e.g. where the Doppler frequency is within an order of magnitude of the power control update, the Rayleigh fading cannot be equalised. In this case, the mobile's  $E_b/N_0$  requirement is essentially that for the Rayleigh fading case, as covered in Section 4.2. An error term arises as the transmitter power level tracks the shadowing dynamics, which is roughly log-normally distributed. This results again in a positive value for  $P_T$ , though this time it is due to the error in tracking shadowing rather than for tracking Rayleigh fading. Simulation results for the standard deviation  $\sigma$  for different diversity conditions and mobile speeds may be found in [25, 26]. Again, the use of STTD to increase the order of diversity will significantly reduce or, especially for  $L = 1$  tap (see Fig. 5 of [26]).

## 5 Algorithm summary and conclusions

This paper has compared the performance of a number of transmit diversity schemes to assess the advantages and disadvantages of each. The STTD scheme provides the best performance of all the techniques which employ no mobile feedback. It provides full dual diversity gain for all coded bits and is compatible with fast power control. If mobile feedback is permitted, the STD and pre-RAKE methods can provide better performance than STTD. However, both techniques are best suited to slowly moving mobiles, in order to minimise the feedback data rate on the uplink. For Rayleigh fading channels, OTD and PSTD are about 0.5–1dB poorer in  $E_b/N_0$  performance than STTD. The PSTD scheme could in principle be applied to existing IS-95 systems without altering the mobile receiver structure. It could thus be seen as an attractive option for retrofitting transmit diversity capability to IS-95 base stations for little additional cost and complexity.

## 6 Acknowledgments

The authors gratefully acknowledge the sponsorship of these studies by the UK EPSRC and Nortel Networks. This paper appeared in part at the IEEE Fall conference on Vehicular Technology, Amsterdam, Holland, Sept 1999.

## 7 References

- 1 The CDMA development group website, URL: <http://www.cdg.org/>.
- 2 GILHOUSEN, K., JACOBS, I., PADOVANI, R., VITERBI, A., WEAVER, L., and WHEATLEY, C.: 'On the capacity of a cellular CDMA system', *IEEE Trans. Veh. Technol.*, 1991, **40**, (2), pp. 303–312
- 3 WALLACE, M., and WALTON, R.: 'CDMA radio network planning'. Proceedings of IEEE international conference on *Universal personal communications* (ICUPC), San Diego, CA, 1994, pp. 62–67
- 4 JALALI, A., and MERKELSTEIN, P.: 'Effects of diversity, power control, and bandwidth on the capacity of microcellular CDMA systems', *IEEE J. Sel. Areas Commun.*, 1994, **12**, (5), pp. 952–961

- 5 WINTERS, J.: 'The diversity gain of transmit diversity in wireless systems with Rayleigh fading', *IEEE Trans. Veh. Technol.*, 1998, **47**, (1), pp. 119-123
- 6 KUO, W., and FITZ, M.: 'Design and analysis of transmitter diversity using intentional frequency offset for wireless communications', *IEEE Trans. Veh. Technol.*, 1997, **46**, (4), pp. 871-881
- 7 TAROKH, V., SESHADRI, N., and CALDERBANK, A.: 'Space-time codes for high data rate wireless communication: Performance criterion and code construction', *IEEE Trans. Inf. Theory*, 1998, **44**, (2), pp. 744-765
- 8 NARULA, A., LOPEZ, M., TROTT, M., and WORNELL, G.: 'Efficient use of side information in multiple antenna data transmission over fading channels', *IEEE J. Sel. Areas Commun.*, 1998, **16**, (8), pp. 1423-1436
- 9 NARULA, A., TROTT, M., and WORNELL, G.: 'Performance limits of coded diversity methods for transmitter antenna arrays', *IEEE Trans. Inf. Theory*, 1999, **45**, (7), pp. 2418-2433
- 10 TIA TR-45.5 SUBCOMMITTEE: The cdma2000 radio transmission technology ITU-R RTT candidate submission, June 1998
- 11 ETSI SMG2: The ETSI UMTS terrestrial radio access (UTRA) ITU-R RTT candidate submission, June 1998
- 12 QUALCOMM INCORPORATED: Proposed EIA/TIA interim standard IS-95, Chapt. 7, April 1992
- 13 VITERBI, A., and OMURA, I.: 'Principles of digital communications' (McGraw-Hill, New York, 1979)
- 14 PROAKIS, J.: 'Digital communications' (McGraw-Hill, New York, USA, 1995, third edn.)
- 15 CLARK, M., GREENSTEIN, L., KENNEDY, K., and SHAFI, M.: 'Matched filter performance bounds for diversity combining receivers in digital mobile radio', *IEEE Trans. Veh. Technol.*, 1992, **41**, (4), pp. 356-362
- 16 SIMPSON, E., and HOLTZMANN, J.: 'Direct sequence CDMA power control, interleaving and coding', *IEEE J. Sel. Areas Commun.*, 1993, **11**, (7), pp. 1085-1095
- 17 NANDA, S., and REGE, K.: 'Frame error rates for convolutional codes on fading channels and the concept of effective  $E_b/N_0$ ', *IEEE Trans. Veh. Technol.*, 1998, **47**, (4), pp. 1245-50
- 18 ALAMOUTI, S.: 'A simple transmit diversity technique for wireless communications', *IEEE J. Sel. Areas Commun.*, 1998, **16**, (8), pp. 1451-158
- 19 HOTTINEN, A., and WICHMAN, R.: 'Transmit diversity by antenna selection in CDMA downlink', Proceedings of IEEE international symposium on *Spread spectrum techniques and applications* (ISSSTA), Sun City, South Africa, September 1998, pp. 767-770
- 20 ANNAMALAI, A.: 'Analysis of selection diversity on Nakagami fading channels', *Electron. Lett.*, 1997, **33**, (7), pp. 548-549
- 21 POVEY, G.: 'Capacity of a cellular time division duplex CDMA system', *IEE Proc. I*, 1994, **141**, (5), pp. 351-356
- 22 COOPER, G., and McGILLEM, C.: 'Probabilistic methods of signal and system analysis' (CBS Publishing, Japan, 1986)
- 23 STUETZLE, R., and PAULRAJ, A.: 'Modelling of forward link performance in IS-95 CDMA networks', Proceedings of IEEE international symposium on *Spread spectrum techniques and applications* (ISSSTA), Mainz, Germany, September 1996, pp. 1058-102
- 24 JALALI, A., FEENEY, M., and CHHEDA, A.: 'Performance of fast forward link power control for CDMA systems', Proceedings of IEEE conference on *Vehicular technology* (VTC), Ottawa, Canada, May 1998, pp. 630-633
- 25 ARIYAVISITAKUL, S., and CHANG, L.: 'Signal and interference statistics of a CDMA system with feedback power control', *IEEE Trans. Commun.*, 1993, **41**, (11), pp. 1624-1634
- 26 NAGUIB, A.: 'Power control in wireless CDMA: Performance with cell site antenna arrays'. Presented at IEEE Globecom conference, Singapore, November 1995

## 8 Appendix: Finite transmit power condition for fast power control

The  $E_b/N_0$  performance of fast power control under the condition that the transmit power  $P_T$  is limited is considered. The noise variance at the receiver is unity, and the channel power  $X$  is modelled as having a PDF  $p(X)$  with unit mean power. The transmitter will then attempt to ensure that the mobile's received  $E_b/N_0$ , denoted as  $P_R$ , is equal to some target  $B$  at all times. The transmitter operates according to the following rule:

$$P_T = \begin{cases} B/X & \text{if } X \geq T \\ B/T & \text{if } X < T \end{cases}$$

where  $T$  represents the maximum power threshold. This means that the maximum transmit power is limited and that the target power  $B$  is attained at the receiver only

when  $X \geq T$ . If  $X < T$ , the transmitter is unable to provide sufficient power to overcome the fading and the received signal power will be smaller than the target  $B$ .

Assume that the frame error ratio function  $F(P_R)$  is known. The FER for any specified value of  $T$  is then given by

$$\text{FER} = \left( \int_T^\infty p(y)dy \right) F(B) + \int_0^T p(y)F(By/T)dy$$

This function can be evaluated to determine the required value of  $B$  to obtain the target FER, which is 1%. The associated mean transmit power is given by

$$E[P_T] = \int_T^\infty \frac{B}{y} p(y)dy + \frac{B}{T} \left( \int_0^T p(y)dy \right)$$

If the fading follows a chi-square distribution of order  $2L$  with unit mean power,  $p(y)$  is

$$p(y) = \frac{L^L}{(L-1)!} y^{L-1} \exp(-Ly)$$

The standard deviation of  $P_T$  is also of importance. It may be found by evaluating the mean square of  $P_T$  as follows:

$$E[P_T^2] = \int_T^\infty \frac{B^2}{y^2} p(y)dy + \frac{B^2}{T^2} \left( \int_0^T p(y)dy \right)$$

The standard deviation is then obtained as

$$\sigma_P = \sqrt{(E[P_T^2] - E[P_T]^2)}$$

If  $T$  is permitted to reduce to zero so that infinite transmitter power is possible, the mean square of  $P_T$  becomes

$$E[P_T^2] = \int_0^\infty \frac{B^2}{y^2} p(y)dy = \frac{B^2 L^2}{(L-1)(L-2)}$$

Using the result for  $E[P_T]$  from the first line of eqn. 9, the standard deviation  $\sigma_P$  is then found to be

$$\sigma_P = \sqrt{\frac{B^2 L^2}{(L-1)(L-2)} - \left( \frac{BL}{L-1} \right)^2}$$

$$= \begin{cases} \infty & L = 1, 2 \\ (BL)/((L-2)^{1/2}(L-1)) & L > 2 \end{cases}$$

This equation shows that increasing  $L$  also reduces the standard deviation  $\sigma_P$ . As an example consider the  $L = 1$  tap Rayleigh fading case. Table 2 presents results for different values  $T$ . The minimum value of the mean transmit power occurs when the maximum allowed transmit power is 20dB above the mean (so  $T = -20$ dB), where  $E[P_T] = 9.9$ dB. As  $T \rightarrow -\infty$  dB,  $E[P_T] \rightarrow \infty$  dB.

Table 2: Results for mean and standard deviation for required transmit power  $P_T$  plotted against  $T$  and  $B$

$T$ (dB)	$B$ (dB)	$E(P_T)$ (dB)	$\sigma_P$ (dB)
0	20.6	19.9	14.3
-10	10.6	15.0	15.4
-20	2.9	9.9	14.0
-30	2.5	11.2	18.9

**This Page is Inserted by IFW Indexing and Scanning  
Operations and is not part of the Official Record**

**BEST AVAILABLE IMAGES**

Defective images within this document are accurate representations of the original documents submitted by the applicant.

Defects in the images include but are not limited to the items checked:

- BLACK BORDERS**
- IMAGE CUT OFF AT TOP, BOTTOM OR SIDES**
- FADED TEXT OR DRAWING**
- BLURRED OR ILLEGIBLE TEXT OR DRAWING**
- SKEWED/SLANTED IMAGES**
- COLOR OR BLACK AND WHITE PHOTOGRAPHS**
- GRAY SCALE DOCUMENTS**
- LINES OR MARKS ON ORIGINAL DOCUMENT**
- REFERENCE(S) OR EXHIBIT(S) SUBMITTED ARE POOR QUALITY**
- OTHER:** \_\_\_\_\_

**IMAGES ARE BEST AVAILABLE COPY.**

**As rescanning these documents will not correct the image problems checked, please do not report these problems to the IFW Image Problem Mailbox.**

**THIS PAGE BLANK (USPTO)**